Core testing method to assess nonlinear behavior of brick masonry under compression A comparative experimental study

Jafari, Samira; Rots, Jan G.; Esposito, Rita

DOI
10.1016/j.conbuildmat.2019.04.188

Publication date
2019

Document Version
Accepted author manuscript

Published in
Construction and Building Materials

Citation (APA)
Jafari, S., Rots, J. G., & Esposito, R. (2019). Core testing method to assess nonlinear behavior of brick masonry under compression: A comparative experimental study. *Construction and Building Materials*, *218*, 193-205. https://doi.org/10.1016/j.conbuildmat.2019.04.188

Core Testing Method to Assess Nonlinear Behavior of Brick Masonry under Compression: A Comparative Experimental Study

Samira Jafari**, Jan G. Rots, Rita Esposito

Delft University of Technology, Faculty of Civil Engineering and Geosciences, Delft, The Netherlands

A B S T R A C T

This study investigates the applicability of the core testing method to assess the complete nonlinear behavior of masonry in compression. A comparative experimental approach was adopted performing compressive tests on cores and companion wallets. Via a correlation study on seven objects, including literature data, a one-to-one correlation for both compressive strength and Young's modulus is obtained, while further studies are necessary to evaluate peak strain and compressive fracture energy. Thanks to its limited invasiveness and the capability of capturing the post-peak response with standard equipment, the core testing method can be regarded as a practical alternative to conventional slightly-destructive techniques.

Keywords:
Cylindrical cores;
Nonlinear compression behavior;
Experimental study;
Slightly-destructive testing method;

1 Introduction

Unreinforced masonry (URM) structures are primarily designed to withstand gravity loads; as a result, their compression characteristics are regarded as fundamental design parameters. As supported by experimental and numerical evidence (e.g. [1-7]), URM under compressive load shows a nonlinear behavior caused by a complex interaction among the masonry constituents (e.g. masonry units and mortar joint) each having different elastic properties. This incompatibility between properties of the masonry units and the mortar under compression leads to the formation of distributed splitting micro-cracks. Upon increasing loads, these micro-cracks grow and coalesce into macro-cracks resulting in localization of deformations and thus masonry failure with energy release from in-plane and out-of-plane splitting, crushing, spalling, interface debonding, friction and shear cracking (e.g. [4-10]).

To experimentally characterize the compression response of brick URM, conventional testing methods regulated by standards [11, 12] can be employed. Following the standards procedure, compression tests can be performed on a small portion of brick masonry, made of minimum two bricks in length and minimum five brick courses in height, either extracted and tested in the laboratory or tested in-situ using flat-jacks. Despite the destructive sampling procedure, which is costly and not always practical, laboratory tests allow for capturing the full nonlinear compression behavior of masonry providing insights into the strength, stiffness and the post-peak softening behavior. The flat-jack tests are less destructive than laboratory tests, but only the elastic response of masonry can

* Corresponding author at: Delft University of Technology, Faculty of Civil Engineering and Geosciences, The Netherlands.
E-mail addresses: S.Jafari@tudelft.nl (Samira Jafari, PhD candidate), J.G.Rots@tudelft.nl (Jan Rots, Professor), R.Esposito@tudelft.nl (Rita Esposito, Assistant Professor)

be captured and insights into the compressive strength as well as the post-peak softening behavior are barely provided. For low value of overburden, due to technical challenges during test execution, uplift of the contrast portion can be expected rather than pressurizing of the masonry portion between the two flat-jacks. Thus, the range of applicability of the flat-jack test is constrained only to walls with high value of the overburden. Results of the flat-jack tests can largely vary when the compressive stress field is not well distributed due to poor quality of masonry or due to cutting operation (e.g. [13-15]). In view of limitations of laboratory destructive tests and in-situ flat-jack tests, the necessity to establish an alternative testing method was widely discussed [16-25].

To overcome limitations of the conventional testing methods, splitting tests on cylindrical cores were recently studied as a promising alternative [18-25]. Small-diameter cores cause limited invasiveness due to sampling and allow testing the samples in laboratory with standard set-up that can grant the possibility of obtaining the complete nonlinear response of masonry beyond the peak strength. This information is essential to provide input parameters for nonlinear finite element analyses based on continuum models (e.g. [26]). According to the method firstly proposed by the International Union of Railways (UIC 778-3R [27]), the masonry compressive strength can be assessed using cores with 150 mm in diameter made of two horizontal (bed) joints and one vertical (head) joint in the center. To apply the compressive load on the core, UIC 778-3R recommends using steel cradles. However, Brencich et al. [18, 19] and Ispir et al. [20] reported no good correlation between the properties obtained from the tests on cores and the ones on companion specimens. This can be caused by the stress concentration, which may arise due to the imperfect contact between the uneven core surface and the steel cradles. To minimizing this effect, Sassoni et al. [21, 22] and Pelà et al. [23] used a high-strength mortar capping placed at the top and bottom of the core. Consequently, a better estimation of the compression properties was achieved. In addition, aiming to minimize the extent of damage due to drilling, Sassoni et al. [21, 22] investigated the suitability of smaller diameter (100 mm) cores. In spite of valuable knowledge gained in the previous studies on the use of the core testing method [18-23], case studies were always limited to clay brick masonry. In most cases, samples were extracted from walls built in laboratory environment, disregarding the possible variability of material properties in existing buildings due to environmental condition, long-term effects and workmanship. In the previous studies, the attention was mainly focused on the characterization of the pre-peak stage, in particular compressive strength and Young's modulus. Less attention was paid to the stress-strain relationship, including the post-peak softening, and its relation to the damage evolution during loading.

The present study aims at evaluating the applicability of the core testing method to assess the complete nonlinear behavior of brick masonry in compression in terms of Young's modulus, compressive strength and the corresponding strain, compressive fracture energy and the stress-strain relationship. A comparative experimental study was conducted at Macrolab/Stevinlaboratory of Delft University of Technology (TU Delft), where cylindrical cores of 150 and 100 mm diameter as well as companion wallets were subjected to compression loading. Prior to testing, cylindrical cores were completed at top and bottom faces using high strength mortar as suggested in previous studies [21-23]. The companion wallets were tested mainly following the EN 1052-1:1998 standard [11],

but a displacement-controlled procedure was adopted.

Four clay and three calcium silicate masonry types were studied, including specimens replicated in the laboratory and extracted from existing buildings. The global response of each case study, compiled from tests on cylindrical cores and wallets, is discussed in details in terms of crack evolution and characteristic of the stress-strain relationships. Primary focus is given to find a correlation between the wallets compression properties and the cores compression properties. For this purpose, a database was created, including the results presented in this paper and literature data.

2 Material and methods

The comparative experimental study included compression tests on cylindrical cores and tests on companion wallets made of the same materials. These samples were either replicated in the laboratory (**Fig. 1**a) or extracted from existing buildings (**Fig. 1**b) located in the northern part of the Netherlands. The latter samples were part of a larger experimental campaign developed at TU Delft for the characterization of the most common Dutch masonry type in support of the hazard and risk assessment of buildings subjected to induced seismicity [28-32]. Accordingly, properties of the masonry constituents of the replicated samples were selected to resemble two typical Dutch masonry typologies [28]: a detached house typology built before 1945 and a terraced house typology built in the period 1960-1980. In the case of the detached house typology, solid clay brick masonry was chosen and both single and double wythe specimens were built. In the case of the terraced house typology, single wythe calcium silicate (CS) brick masonry was selected being representative of the inner leaf of the typical cavity wall system. The masonry samples replicated in the laboratory showed a uniform texture by controlling the construction process, in which the influence of workmanship was limited as much as possible. To replicate clay masonry, solid clay bricks having nominal dimensions of 210x50x100-mm and commercial pre-mixed mortar with a cement:lime:sand ratio by volume of 1:2:9 were used. In this study, to build the single wythe clay masonry (MAT-3) and double wythe clay masonry (MAT-4) specimens, the same materials were adopted. To replicate calcium silicate masonry, calcium silicate bricks having nominal dimensions of 210x70x100-mm and a pre-mixed mortar with a volume ratio of cement to sand as 1:3 were used. The used bricks (i.e. solid clay or CS) as well as pre-mixed mortars were all selected from a single production batch. These choices were made to minimize the variation of the material properties, since these tests served as part of a larger campaign, where behavior of masonry at component [33, 34] as well as structural level [35] was investigated.

To extract cylindrical cores and wallets from the existing buildings, the prescription of the ASTM C1532 [36] was followed. First, each building was inspected and the potential locations of sampling were identified. Second, the samples were taken out from walls using a dry extraction procedure. Eventually, each extracted sample was fully packed and transported to the laboratory.

Treating each masonry type replicated in the laboratory and each building as a separated object, in total, seven testing objects were investigated in this study. Table 1 lists an overview of the tested masonry objects, specifying

unit type (solid clay or CS brick), number of wythe (single or double) and construction conditions (obtained from masonry replicated in the laboratory or extracted from existing buildings). The single wythe specimens, with a thickness of 100 mm, were made with a running bond, while double wythe specimens, with a thickness of 210 mm, were made with Dutch bond.

The flexural and compression characteristics of the mortar used in the construction of the replicated objects were determined from tests on mortar bars according to the EN 1015-11:1999 standard [37]. The flexural strength was assessed by a three-point bending test on mortar bars with 40x40x160-mm, while compressive strength was determined from tests on broken specimens previously tested in the bending configuration. **Table 1** lists the flexural strength and the compressive strength of the mortar tested at least 28 days after casting; the coefficient of variation is indicated in parentheses. The flexural strength and compressive strength of mortar for the CS brick masonry (MAT-1) are approximately 2 times higher than the corresponding values for the clay masonry specimens (i.e. MAT-3 and MAT-4). In the case of existing objects, the mortar properties could not be investigated due to difficulties of extracting intact mortar samples.

Both for replicated and existing objects, the flexural and the compressive strength of bricks were evaluated according to the NEN 6790:2005 [38] and EN 772-1:2000 [39] standards, respectively. The mean value of the brick flexural strength was determined with three-point bending tests on six bricks; the load was applied parallel to the bed joint plane of the brick. A linear behavior was observed approximately up to 90% of the peak load; subsequently some nonlinearity occurred just before the peak, followed by a brittle failure at maximum force. The compressive strength of brick was evaluated while load was applied perpendicular to the bed joint plane. The normalized mean value of the brick compressive strength was calculated from tests on six bricks, considering the shape factor accounting for the height-to-thickness ratio. The brick flexural strength and normalized compressive strength are given in **Table 1**. The flexural strength of clay bricks used to replicate samples in the laboratory (MAT-3 and MAT-4 objects) was approximately 2 times higher than the other brick types. A high dispersion of the flexural strength with 76% coefficient of variation was found for the bricks extracted from the Molenweg object. The highest normalized compressive strength belonged to the clay brick from the Rengersweg object amounting to 41.90 MPa and the lowest normalized compressive strength was obtained for the CS brick from the MAT-1 object with the mean value of 13.26 MPa. The dispersion of the compressive strength of the existing objects was relatively low as the coefficients of variation ranged between 12% and 17%, less than for individual brick flexural strength ranged between 29% and 76%. Due to limitation of sampling area in existing buildings, single CS bricks could not be extracted from the Tilweg object; in the case of Rengersweg object, six intact bricks were extracted and only tested in compression.

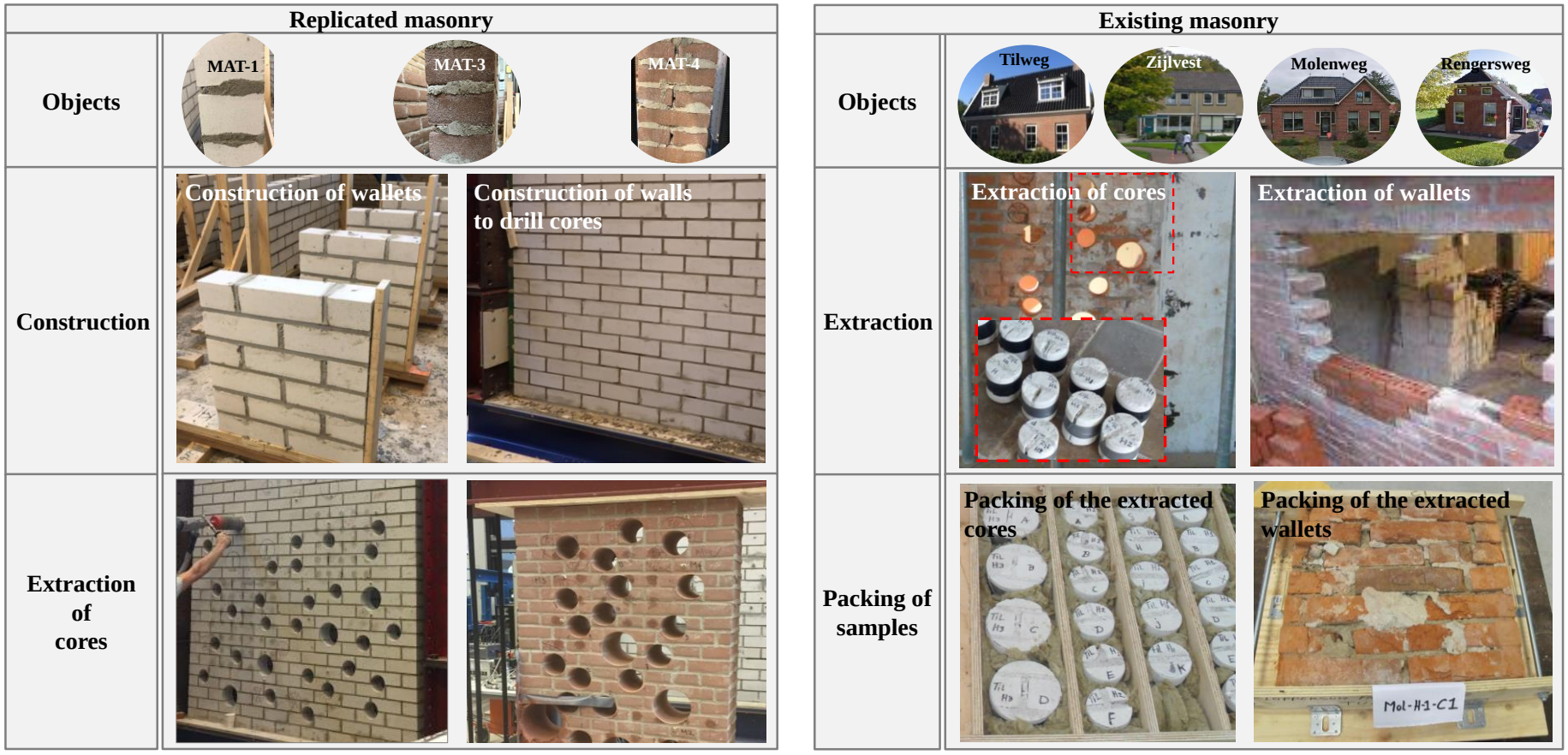

Fig. 1. Overview of the masonry objects: (a) replicated in laboratory; (b) extracted from existing buildings.

Table 1

Overview of the tested masonry objects including mortar and brick properties, wallet dimensions and length of LVDTs.

Name objects	Brick types	No. of wythe	Replicated/ Existing*	Mortar properties**		Brick properties**		Wallet size and LVDTs length ***			
				Flexural strength MPa	Compressive strength MPa	Flexural strength MPa	Compressive strength MPa	Size of wallets mm^3	A mm	B mm	C mm
MAT-1	CS	Single	Replicated	3.21 (5%)	7.57 (6%)	2.79 (11%)	13.26 (13%)	434x476x100	243	332	298
Tilweg	CS	Single	Existing (2000)	-	-	-	-	450x490x100	250	330	290
Zijlvest	CS	Single	Existing (1976)	-	-	3.53 (29%)	15.90 (17%)	460x420x100	145	210	330
MAT-3	Clay	Single	Replicated	1.40 (12%)	3.81 (9%)	6.31 (11%)	28.31 (10%)	430x470x100	300	330	290
MAT-4		Double						540x650x210	360	390	290
Molenweg	Clay	Single	Existing (1932)	-	-	2.78 (76%)	21.73 (13%)	475x433x117	200	220	200
Rengersweg	Clay	Single	Existing (1920)	-	-	-	41.90 (12%)	450x270x100	85	225	-

* Year of construction of the existing building is indicated in parentheses.

**Coefficient of variation is indicated in parentheses.

*** For definition of parameters A, B and C see **Fig. 2**c.

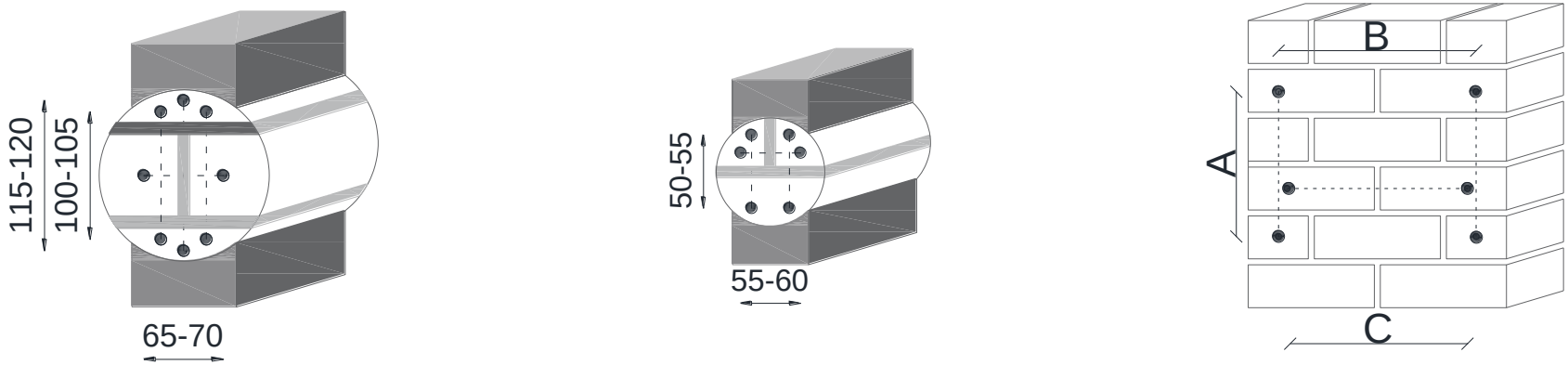

(a) (b) (c)

Fig. 2. Overview of specimen geometry and LVDTs arrangement: (a) H-shaped core with 150 mm diameter; (b) T-shaped core with 100 mm diameter; (c) companion wallets. The length of parameters A, B and C is given in Table 1.

2.1 Specimen geometries

The comparative experimental study included tests on cores, with 150 and 100 mm diameter, as well as tests on companion wallets, with minimum two bricks in length and minimum five brick courses in height. In the thickness, the specimens were either 100 mm (single wythe with running bond) or 210 mm (double wythe with Dutch bond).

Two core types were adopted: H-shaped core with a diameter of 150 mm and T-shaped core with a diameter of 100 mm. The former consisted of two bed joints and one central head joint (**Fig. 2**a), while the latter was formed of one central bed joint and one head joint (**Fig. 2**b). The masonry cores were extracted perpendicular to the wall surface, using a dry extraction procedure as suggested by Pelà et al. [23]. To preserve the integrity of the replicated walls during the sampling procedure, they were pre-compressed using pre-stressed rods. Generally, for replicated clay masonry (MAT-3 and MAT-4) in some cases a wet extraction procedure was adopted due to technical issues.

To evenly distribute the compressive load on the cross-sectional area of the cylindrical cores and to avoid stress concentration which may be caused due to irregular surface of the core, cylindrical cores were capped at top and bottom using high strength mortar (see **Fig. 2**a,b). This procedure, first proposed by Sassoni et al. [21, 22] and subsequently applied by Pelà et al. [23], differs from the one proposed by the UIC 778-3R [27] in which the steel cradles are used to distribute the load. Following this procedure, a good bond between the cap and the core was reported, moreover, a confinement effect experienced in a real wall was simulated [21, 22]. In this study, a high strength mortar showing a brittle behavior under compression was used for capping. To evaluate the compression properties of the capping mortar, mortar bars were cast in molds and kept in laboratory conditions under ambient conditions. Compression tests on the mortar bars were performed 3, 7, 10 and 28 days after casting. Following the EN 13412:2006 [40] standard, the compressive strength and the Young's modulus of the capping mortar were evaluated as 60 MPa and 34 GPa, respectively; 95% of the cap strength was achieved after 3 days. Note that the capping mortar should have enough workability to create a continuous bond with the brick [41]. After capping, cylindrical cores were kept in laboratory conditions. The caps were unmolded after at least 1 day; testing took place at least after 7 days.

To validate the applicability of the core testing method, companion wallets were subjected to compression loading. Following prescriptions of the EN 1052-1:1998 standard [11], dimensions of the companion wallets depend on the size of brick and on the number of wythes (i.e. single or multiple wythe). However, due to difficulties of extracting large samples from existing buildings, only wallets from the Tilweg object had a height according to the standard prescriptions. Similar to the core samples, a dry extraction procedure was adopted to take wallets out of existing buildings. All the wallets replicated in laboratory were constructed on wooden frame to facilitate handling. The wallets dimensions are specified in **Table 1**. To ensure that the loaded faces of the wallets were leveled and parallel to each other, as suggested by the standard, a 10-mm thick layer of gypsum was applied to the faces in contact with the loading plates.

2.2 Testing set-ups and procedures

A displacement-controlled procedure was applied to capture the nonlinear behavior up to and beyond the peak. The cylindrical cores and companion wallets were tested using a compression test set-up with a 3500 kN hydraulic jack. The peak load of the specimens was reached between 15 and 30 minutes, following the prescriptions of the EN 1052-1:1998 standard. The vertical and horizontal deformations both on the front and on the back side of the specimens were continuously measured using Linear Variable Differential Transformers (LVDTs). The LVDTs had a measuring range of 10 mm and accuracy of ±1 μm. Each face of the cylindrical cores and of the wallets was equipped with two vertical LVDTs and one horizontal LVDT (**Fig. 2**a,b). For the cores, the length of the LVDTs was kept almost unchanged, while for the companion wallets it varied based on the wallet dimensions (**Fig. 2**c and **Table 1**). In the latter case, aiming for a better estimation of the compressive fracture energy, the length of the vertical LVDTs was generally higher than the one prescribed (EN 1052-1:1998). No rotation or buckling of the vertical LVDTs in the pre-peak phase was reported. On the contrary, for large out-of-plane or in-plane post-peak deformations of specimen, rotation and detachment of the LVDTs were observed, thus, the corresponding readings were not taken into account. In order to obtain the stress-strain relationship for the post-peak phase, readings of the hydraulic jack were used. The vertical displacement of the jack had the same trend of the LVDTs and a linear relationship was observed between them. The full stress-strain relationship was obtained in the pre-peak phase by the LVDTs readings and in the post-peak phase by the jack's readings applying a scalar factor, which allows obtaining the same peak displacement (**Fig. 3**a). The axial strain and the lateral strain were calculated as an average of the strains of all individual vertical and horizontal LVDTs, respectively.

In this study, the compressive behavior of masonry is characterized in terms of Young's modulus, compressive strength and corresponding peak strain, and compressive fracture energy; an analysis of the stress-strain relationships for axial (i.e. vertical LVDTs reading) and lateral strain (i.e. horizontal LVDTs reading) are provided. The Young's modulus (E) was evaluated between 1/10 and 1/3 of the maximum stress, aiming to eliminate an initial start-up of the stress-strain curve usually caused by the gradual contact between loading plates and specimen, and thus, may unrealistically affect the estimation of the elastic modulus. This initial adjustment between the machine plates and the specimen was also observed by García et al. [42], during compression tests on stone masonry. The compressive strength (f'_m) was determined as a ratio between the failure load and the loaded cross-sectional area of the individual specimen. In the case of core, the loaded cross-sectional area can be referred to the horizontal maximum cross-section (according to UIC 778-3R) or to the cap cross-sectional area (as proposed by Pelà et al. [23]); in this study the latter is considered. The peak strain was determined as the strain corresponding to the peak load. In order to describe the gradual post-peak softening, the concept of compressive fracture energy introduced by van Mier [8] for concrete and further used by Lourenco [5] for masonry was adopted. The compressive fracture energy was calculated as the area underneath the stress-axial displacement curve over the height of the masonry specimen (thus excluding the cap's height in the case of core). To obtain the ultimate displacement, the post-peak

softening branch was approximated with a linear relation after reaching a stress level of 0.3 f'_m, the slope of this line was evaluated between 0.5 f'_m and 0.3 f'_m (**Fig 3**b). Considering the elastic-brittle behavior of the capping mortar (explained in Section 2.1), it was assumed that no energy was dissipated by the capping mortar and the energy dissipation was caused only by the fracture process in the masonry.

To compare the stress-strain relationships obtained from tests on cylindrical cores and companion wallets, the mean stress-strain curves, considering the axial and lateral strains, were derived for each object following the approach proposed by Augenti et al. [43]. For all individual masonry objects, the mean stress-strain curve was obtained by considering pre-defined increments of axial strain and calculating the corresponding average stress as well as the corresponding average lateral strain. In this study, an increment of the axial strain equal to 1.5E-05 ± 1% was chosen.

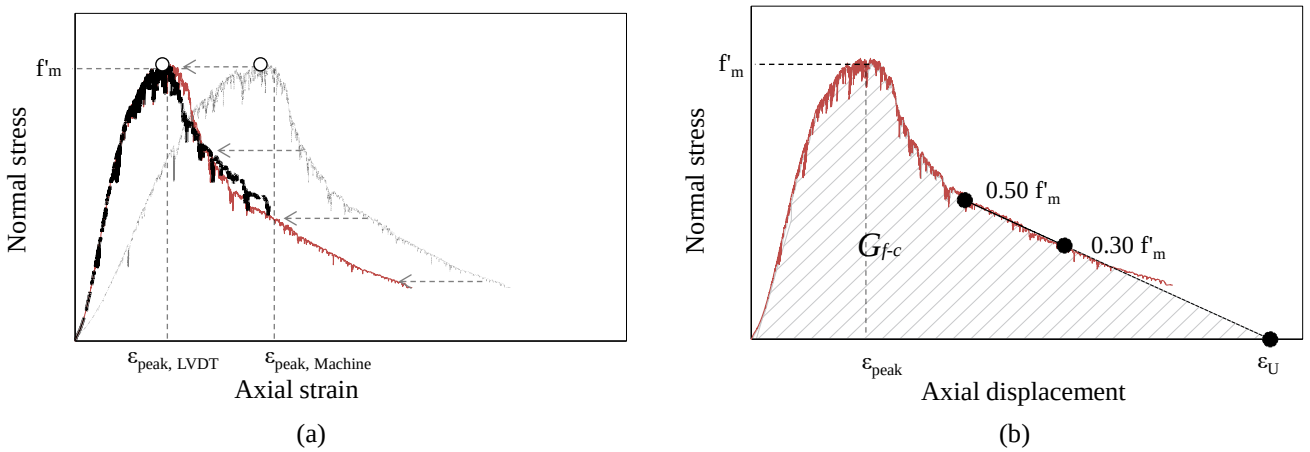

Fig. 3. Compression test: (a) obtaining full stress-strain curve from LVDTs' and jack's reading; (b) estimation of compressive fracture energy ($G_{f\text{-}c}$) from stress-axial displacement curve.

3 Global behavior

In this section the global response of cores, both with diameter of 150 and 100 mm, and companion wallets under compression load is described in terms of crack patterns and shape of the stress-strain relationships. First, the relation between the stress-strain relationships and the observed crack pattern is presented. Second, observations of the confinement effects due to the capping mortar on the core behavior are presented comparing the axial strain versus lateral strain curves. Eventually, an overview of the behavior of each object is separately presented. Note that an overview of the obtained material properties for cores and wallets is given in Section 4, where the correlation study is discussed.

3.1 General response

The general response of the cores and wallets is presented by correlating the stress-strain relationships with the evolution of crack pattern (**Fig. 4**). The analysis was carried out considering 3 phases: an initial linear-elastic phase, a pre-peak hardening phase and a post-peak softening phase.

Initial linear-elastic phase: For the cores, a linear-elastic relation was observed between the stress and the axial

strain up to approximately 40% of the compressive strength; no visible crack was detected on the core faces. However, reduction of lateral stiffness was observed (**Fig. 4**a), which can imply that internal micro-cracks were formed. For the wallets, no reduction of axial stiffness was observed approximately up to 50% of the compressive strength. However, the first sign of cracking was observed either along the brick-mortar interface of head joints or as vertical splitting cracks in the bricks followed by a small reduction in the lateral stiffness. In this phase, an acceptable match was found between the slopes of the stress versus axial strain curve, the so-called Young's modulus, obtained from tests on the cores and from tests on wallets. On the contrary, the lateral stiffness of the cores was reported approximately 3 to 5 times lower than the one of the wallets.

Pre-peak hardening phase: Following the initial linear-elastic phase, both cores and wallets showed a hardening phase up to the peak strength, but a different crack pattern was observed. In the case of cores, the first vertical splitting crack often appeared along the brick-mortar interface of the head joint. As load being increased, more vertical splitting cracks spread in the specimen and were often localized close to the boundaries of the cap; no crushing or spalling was observed. In the case of wallets, the vertical tiny cracks, already were appeared in the initial phase, gradually increased their length. In addition, vertical splitting cracks, uniformly spaced along the length and width of wallets; mortar crushing of the bed joints were also observed. For the stress level of 90% of the compressive strength, surface spalling along the length of wallets was also detected. Generally, the values of the axial peak strain obtained for the cores, both 150 and 100 mm in diameter, were up to 3 times higher than the peak strain values obtained for the wallets. The CS masonry cores and wallets showed a longer hardening regime with respect to clay masonry specimens. This can result from gradual splitting process of the CS bricks and a stronger mortar as compared to the clay masonry.

Post-peak softening phase: Both cores and wallets showed a post-peak softening behavior; a change in the slope of the curve was often observed at a residual stress of 90-85% of the compressive strength. The tests were terminated when the specimens were fully disintegrated and no more mechanical damage was reported due to friction. In the case of cores, the widening of the previously formed cracks was observed rather than the development of new cracks at close spacing. The localized vertical cracks aligned with the boundaries of the cap fully developed along the height and the width of the cores and thus led to the detachment of the marginal parts of the masonry that were not originally in contact with the cap. In the case of wallets, explosive splitting cracks (in particular for clay wallets) and spalling on the face of the wallets at the center were often reported. In some cases along the width of wallets, in-plane branching cracks having a "V-shape" or shearing cracks triggering a sliding between the front and back face of the wallets were observed.

The compression properties of the cylindrical cores can be evaluated either by considering the horizontal maximum cross-sectional area of the core or of the cap. As mentioned earlier, vertical splitting cracks in the cores generally localized at positions underneath the boundaries of the cap. This localization often led to the detachment of the external part of the core. In agreement with the observed crack pattern, all the compression properties of the cylindrical cores were evaluated considering the cross-sectional area of the cap, although not all the cores showed

localized cracks along the outer edges of the cap.

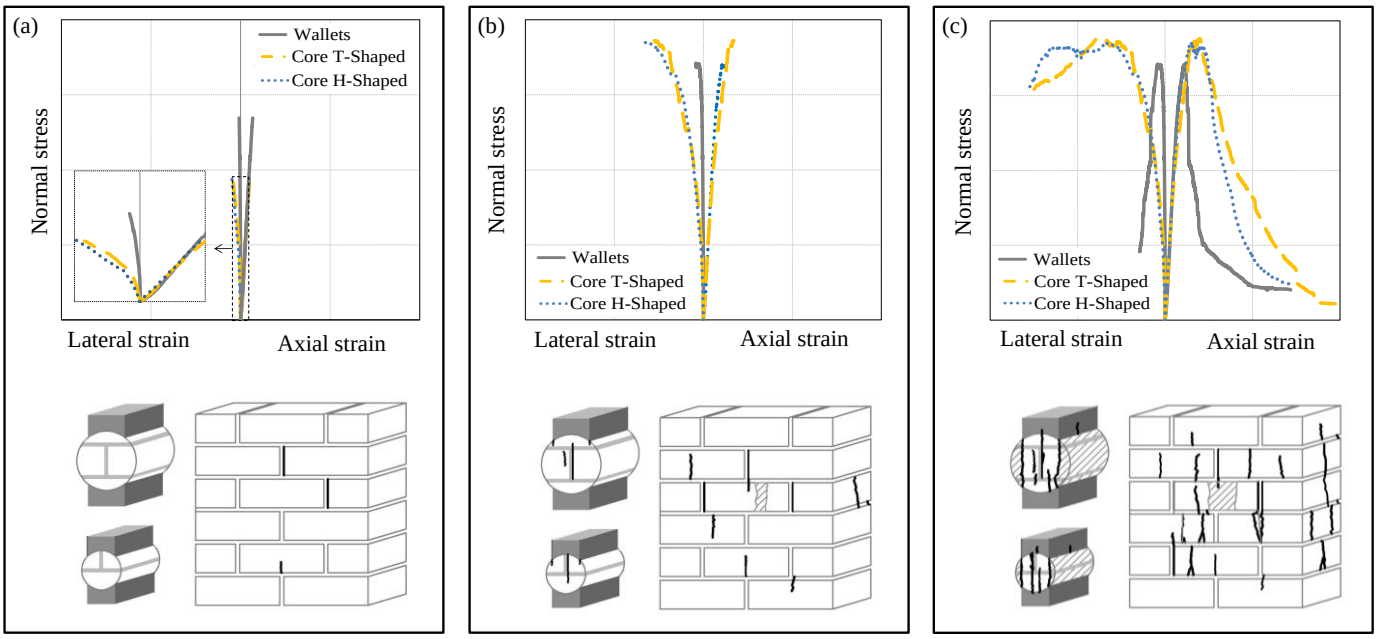

Fig. 4. Typical compression response at three different phases: (a) initial linear-elastic phase; (b) pre-peak hardening phase; (c) post-peak softening phase. The shaded areas indicate detachment of material in cores and spalling in wallet.

To evaluate the effect of the difference in boundary conditions between cores and wallets, the typical stress versus axial displacement and axial strain versus lateral strain curves are analyzed in **Fig. 5**. The wallets showed a more ductile post-peak phase caused by less localized cracks with respect to the cores. Additionally, the T-shaped cores showed more brittle and more localized cracks than the H-shaped ones. Due to the frictional constraint between the masonry core and the capping mortar, it can be assumed that cores were generally more constrained than wallets. Higher peak strain was found for the cores in both axial and lateral directions with respect to the wallets. The ratio in terms of peak axial strain values between T-shaped and H-shaped cores for different objects varied between 0.6 and 1.6, while comparing the cores and the wallets a variation between 0.31 and 1.0 was found (**Fig. 5**b). Further research is ongoing to evaluate the possible influence of the cap stiffness and the cap geometry on evaluation of the compression properties.

The evolution of cracks in the capping mortar was closely inspected to detect any undesired premature cracking of the capping mortar. Being a stiffer capping mortar bonded to a softer masonry core, cracking in the cap is expected due to the difference in stiffness of the two materials for large vertical displacements [4] (**Fig. 6**a). However, onset of cracking is expected in the masonry core. In few cases, a premature vertical crack, located at half the width of the cap, was observed in the capping mortar. During the curing period, an uneven top surface of the cap was often observed, which could be the cause for the premature cracking of the capping mortar during the compressive test. In the case that an uneven surface was observed, a finishing layer of gypsum was applied to restore the flat surface. This procedure was applied only in the case of cores extracted from existing structures. For the cores extracted from replicated walls, prior to the test, irregularity in the capping surface was not carefully

investigated; consequently, a post evaluation was carried out based on photographic documentation. **Fig. 6**b shows the influence of premature cracking in terms of stress-axial strain relations. The compressive strength was hardly affected by the premature cracking of the cap, while it often provided an underestimation of the Young's modulus and an overestimation of the peak strain as well as the compressive fracture energy. Accordingly, for specimens with first sign of cracking in the cap, only compressive strength values were taken into account and the other properties were excluded in the calculation of the mean values reported in Section 4.

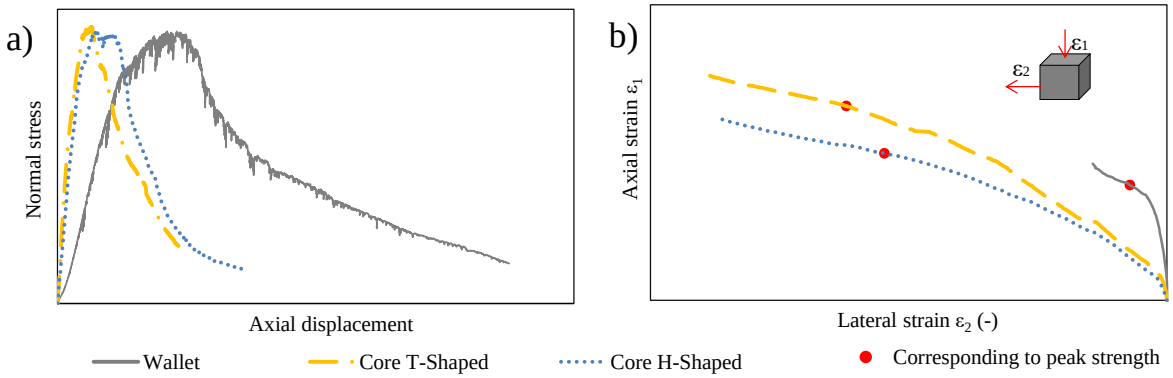

Fig. 5. Confinement effect in cores and in wallets: (a) typical stress-axial displacement curves; (b) typical axial strain-lateral strain curves.

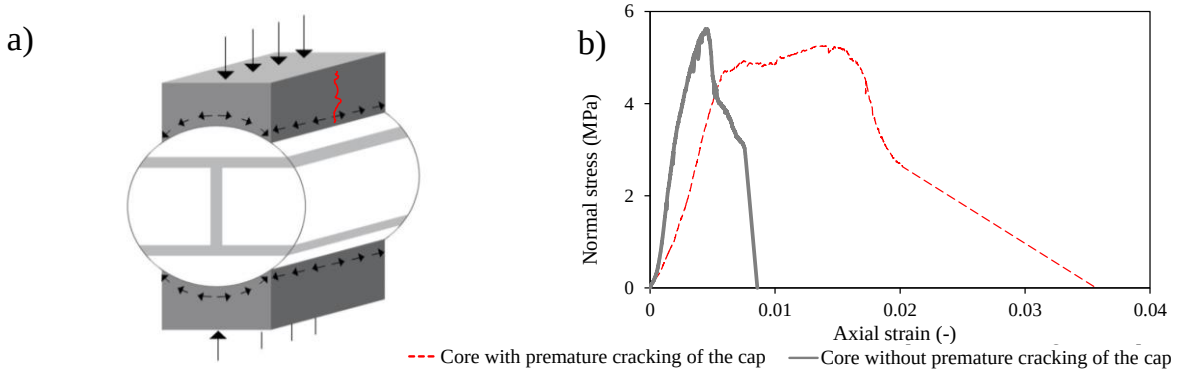

Fig. 6. (a) Premature cracking of the capping mortar; (b) difference between compression response of masonry cores with and without premature cracking in the cap.

3.2 Response of each masonry object

In this section, the response of cores and companion wallets is analyzed per each masonry object in **Fig. 7** to 13. Each figure is composed of six parts, namely: (a) crack pattern of the wallets; crack pattern of the T-shaped cores (b) front view and (c) side view; crack pattern of the H-shaped cores (d) front view and (e) side view and (f) mean stress-strain curves for the wallets (grey line), T-shaped (yellow line) and H-shaped (blue line) cores. Due to limited data on wallets for the Rengersweg object, the mean stress-strain curve was approximated as a linear curve in the pre-peak phase (**Fig. 13**f). In this section, those objects that showed a response different from the general trend (described in Section 3.1) are further analyzed. This analysis is performed in view of the correlation study, which will be presented in Section 4.

For the replicated CS masonry cores (MAT-1), the cracking occurred in the cap rather than in the masonry. As

expected, the cores showed lower stiffness and higher peak strain with respect to the masonry wallets (**Fig. 7**f). Consequently, for this object only compressive strength values can be regarded as reliable.

The compressive strength of the double wythe clay masonry (MAT-4) was overestimated by 63% using the core method (**Fig. 11**f). This difference in the compressive strength may result by the excessive confinement of the lateral expansion along the width of the core caused by the cap. The presence of a continuous cap might not allow the opening of the central joint in the width of the core, while this phenomenon was observed for the wallets. Further studies are necessary to investigate this phenomenon and its influence on the compressive properties of masonry. Accordingly, the correlation study presented in following section only focuses on single wythe specimens.

The compressive strength of the existing clay masonry extracted from the Molenweg object was overestimated by 84% using the core method (**Fig. 12**f). Visual inspections of the Molenweg building indicated pre-existing cracks in the bricks and only partial filling of the joints, which resulted in very low value of the wallets compressive strength (4.00 MPa). This non-uniform texture of the Molenweg object was caused probably due to poor workmanship and aging. In case of irregular masonry, unbiased sampling is not always achievable. In order to ensure the integrity of the core, it may be assumed that cores were extracted from “best pieces”, while for the larger wallets biased sampling was not possible. Therefore, the properties obtained from the core testing method may not be representative.

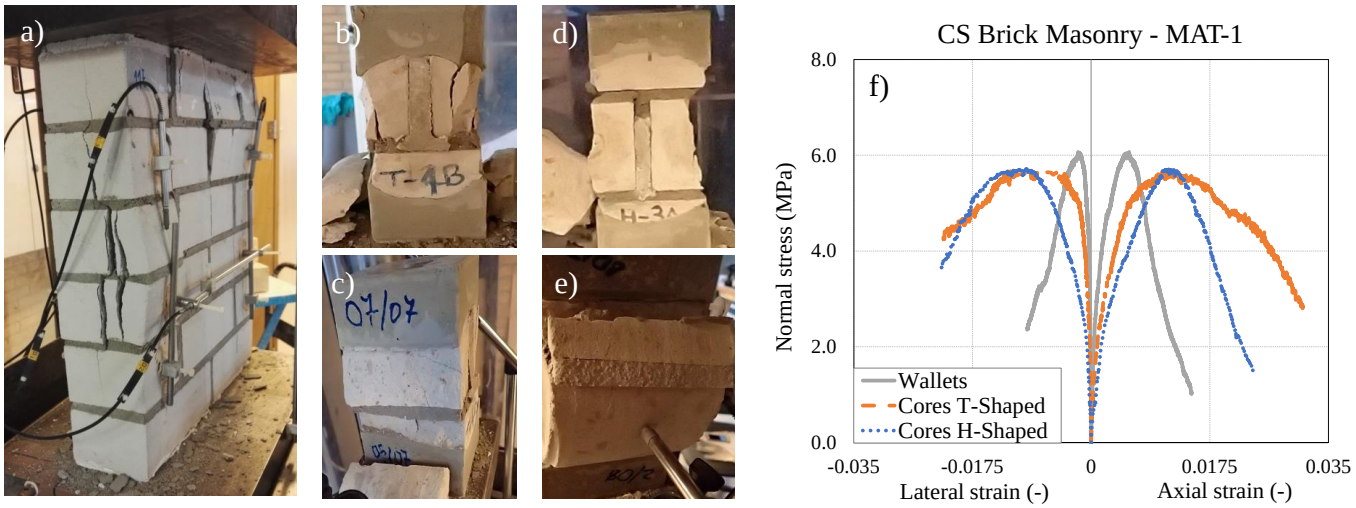

Fig. 7. Replicated calcium silicate masonry (MAT-1): (a) final crack pattern of wallets; (b)-(c) final crack pattern of T-shaped core; (d)-(e) final crack pattern of H-shaped core; (f) mean stress-strain relationships.

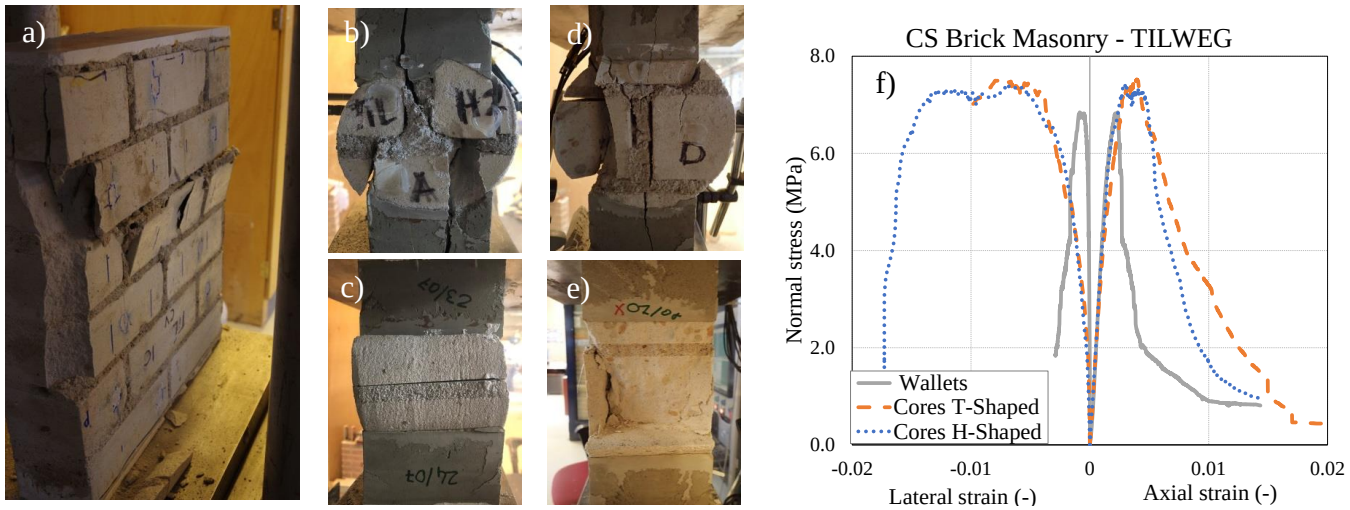

Fig. 8. Existing calcium silicate masonry (Tilweg): (a) final crack pattern of wallets; (b)-(c) final crack pattern of T-shaped core; (d)-(e) final crack pattern of H-shaped core; (f) mean stress-strain relationships.

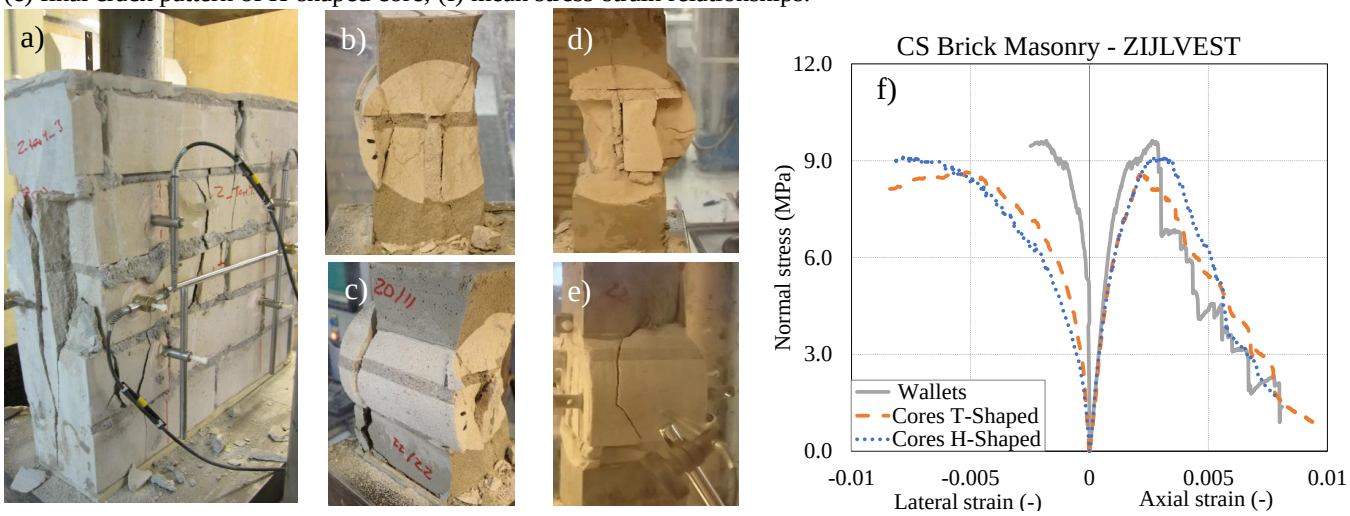

Fig. 9. Existing calcium silicate masonry (Zijlvest): (a) final crack pattern of wallets; (b)-(c) final crack pattern of T-shaped core; (d)-(e) final crack pattern of H-shaped core; (f) mean stress-strain relationships.

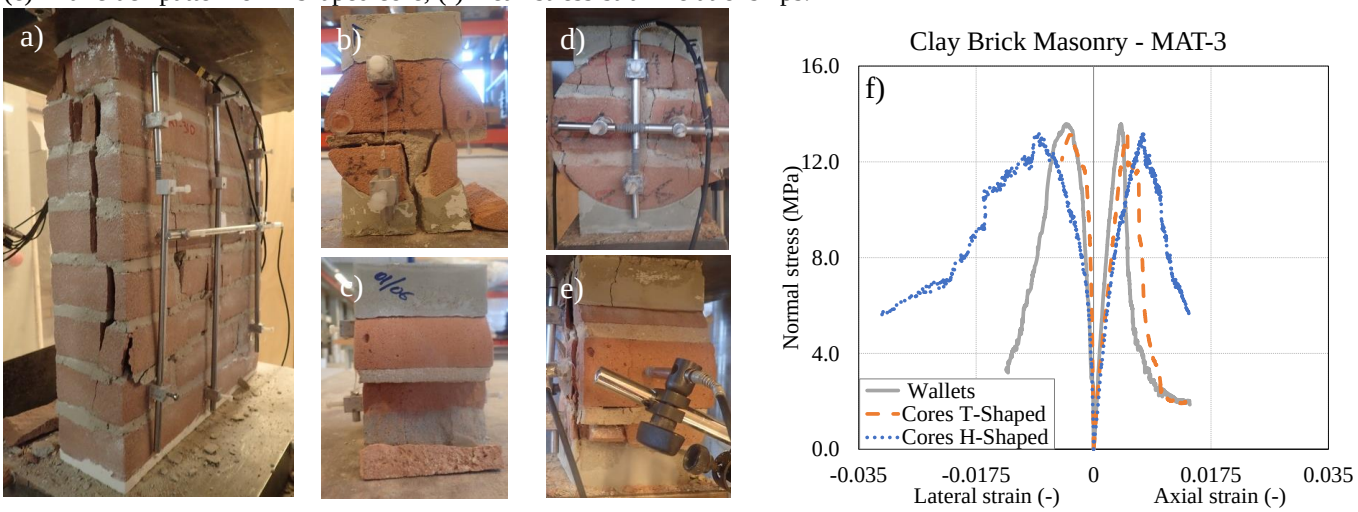

Fig. 10. Replicated clay masonry (MAT-3): (a) final crack pattern of wallets; (b)-(c) final crack pattern of T-shaped core; (d)-(e) final crack pattern of H-shaped core; (f) mean stress-strain relationships.

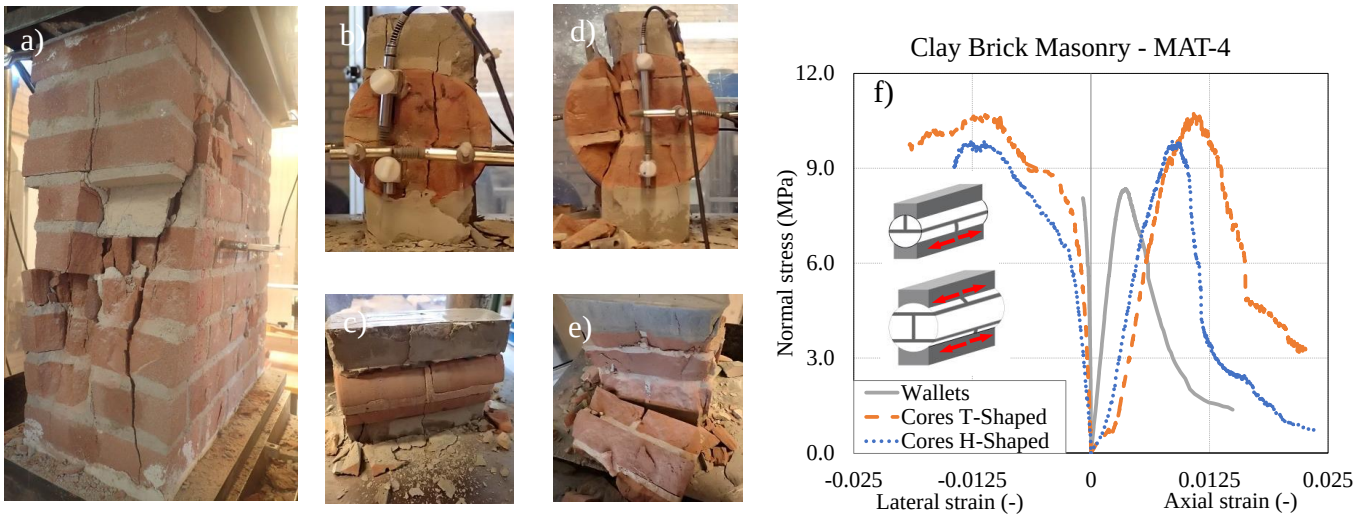

Fig. 11. Replicated clay masonry (MAT-4): (a) final crack pattern of wallets; (b)-(c) final crack pattern of T-shaped core; (d)-(e) final crack pattern of H-shaped core; (f) mean stress-strain relationships.

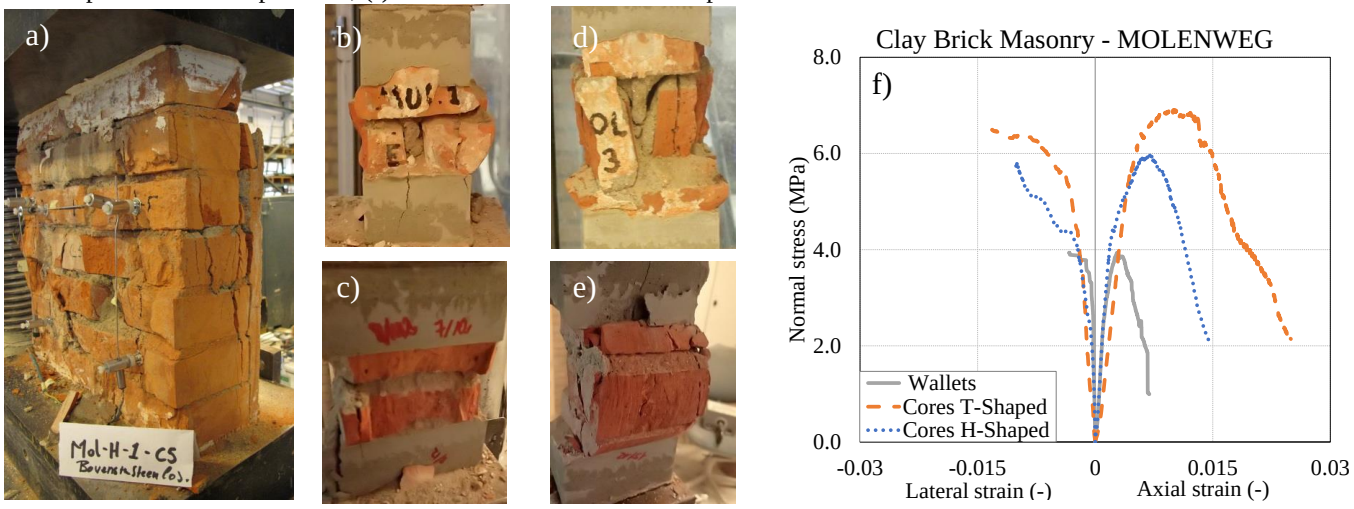

Fig. 12. Existing clay masonry (Molenweg): (a) final crack pattern of wallets; (b)-(c) final crack pattern of T-shaped core; (d)-(e) final crack pattern of H-shaped core; (f) mean stress-strain relationships [44].

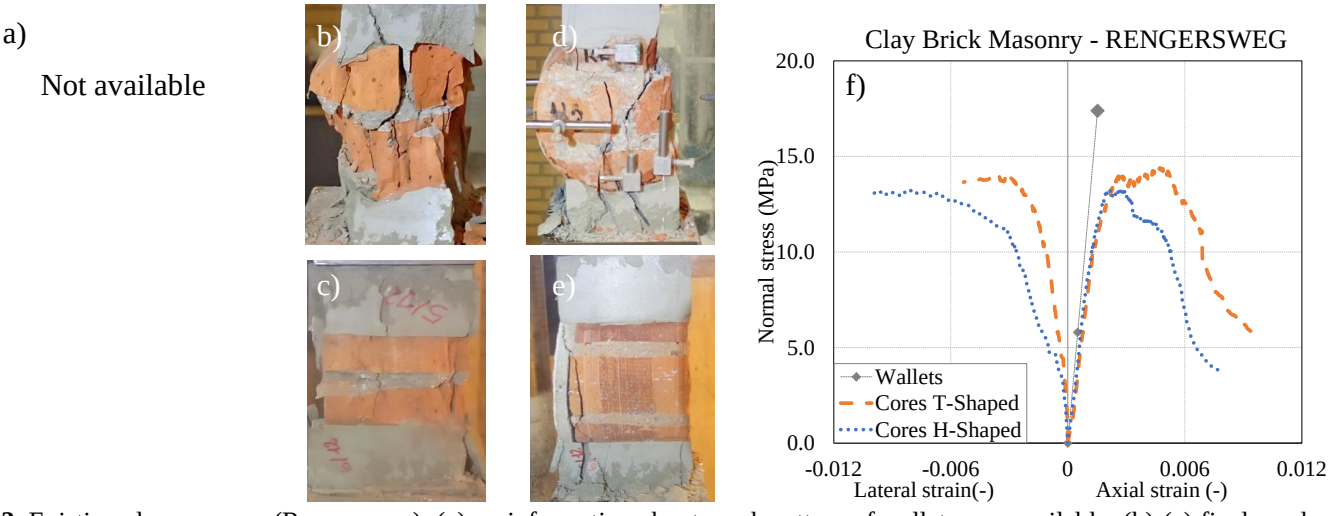

Fig. 13. Existing clay masonry (Rengersweg): (a) no information about crack pattern of wallets was available; (b)-(c) final crack pattern of T-shaped core; (d)-(e) final crack pattern of H-shaped core; (f) mean stress-strain relationships [45].

Table 2

Database of compression tests on cores and companion specimens.

Name / Ref	Unit[1]	No. Wythe[2]	Characteristic of cylindrical cores								Characteristic of companion specimens					
			No. Spec.	$Area_{core}/Area_{cap}$	Height of cap	D_{core} mm	$f'_{m,core.}$ MPa	E_{core} MPa	$\varepsilon_{peak,core}$ ‰	$G_{f\text{-}c,core}$ N/mm	No. Spec.	Size No.brick	f'_m MPa	E MPa	ε_{peak} ‰	$G_{f\text{-}c}$ N/mm
MAT-1	CS/R	S	6	1.3	30	94	6.17	1674	18.73	14.92	6	2x6x1	6.35	4265	5.90	20.03
MAT-1	CS/R	S	6	1.6	29	143	6.18	1172	14.10	13.73						
Tilweg	CS/E	S	5	1.3	44	93	7.68	4515	3.85	5.46	3	2x6x1	6.93	4460	2.25	11.52
Tilweg	CS/E	S	5	1.6	45	144	8.37	4634	3.24	7.18						
Zijlvest	CS/E	S	7	1.3	43	94	9.38	9674	2.41	3.17	3	2x5x1	9.86	8639	2.44	15.95
Zijlvest	CS/E	S	7	1.6	49	144	9.52	8078	2.84	6.25						
MAT-3	C/R	S	2	1.3	24	100	13.00	3066	4.79	10.97	6	2x8x1	14.02	4590	4.26	29.34
MAT-3	C/R	S	2	1.5	20	150	14.04	2974	8.55	17.79						
MAT-4	C/R	D	6	1.4	35	100	15.08	2547	12.69	14.81	12	2x10x2	9.56	2951	4.06	33.27
MAT-4	C/R	D	5	1.7	41	150	13.76	2422	9.78	19.09						
Molenweg*	C/E	S	5	1.4	44	95	7.38	2205	5.08	10.49	3	2x7x1	4.00	3167	2.95	10.37
Molenweg*	C/E	S	6	1.6	49	144	6.36	2743	5.88	9.67						
Rengersweg*	C/E	S	6	1.4	41	95	17.51	10268	3.64	6.60	3	2x5x1	17.39	11390	-	-
Rengersweg*	C/E	S	6	1.6	48	144	14.70	10749	2.30	9.10						
ARCH [21]	C/E	S	9	1.2	40	100	15.88	-	-	-	3	2x3x1	13.20	-	-	-
MT1 [22]	C/R	D	9	1.3	40	100	12.69	-	-	-	3	3x12x2	8.47	-	-	-
MT2 [22]	C/R	D	14	1.3	40	100	17.06	-	-	-	3	3x12x2	10.23	-	-	-
3JC [23]	C/R	S	6	1.4	-	150	8.40	2570	-	-	6	1x5x1	5.82	2855	-	-

[1] Unit: CS/R = Calcium silicate masonry replicated in laboratory; C/R = Solid clay masonry replicated in laboratory;
CS/E = Calcium silicate masonry extracted from existing buildings; C/E = Solid clay masonry extracted from existing buildings;

[2] No. wythe: S = Single wythe; D = Double wythe.

* Tests on companion wallets were performed by third parties [44, 45].

Excluded from correlation study

4 Correlation study

To evaluate the reliability of the core testing method, a correlation study is performed including the data presented in this paper and the ones presented by Sassoni et al. [21, 22] and Pelà et al. [23]. Although other references are available in literature regarding core testing method (e.g. [18-20]), in this study the attention is focused only on cores made with at least one vertical head joint and capped with high strength mortar (**Table 2**). Cores without any vertical head joint were omitted, because they could not represent the failure mode of the companion wallets; in particular, when the onset of cracking is located in the head joint rather than in the brick. Sassoni et al. [21, 22] studied the applicability of masonry cores with 100 mm in diameter to reproduce the compressive strength of companion wallets for three masonry objects. Pelà et al. [23] replicated a single wythe masonry object comparing results of tests on cores with a diameter of 150 mm and tests on companion prisms.

Table 2 lists the compressive properties for every analyzed object in terms of Young's modulus, compressive strength, peak strain and compressive fracture energy of both cylindrical cores and companion wallets. The number of tested cores and tested companion wallets, the ratio between the horizontal maximum cross-sectional area of the core (A_{core}) and of the cap (A_{cap}), the minimum height of the cap at its center, the core diameter (D) and the dimension of the companion specimens are listed. In **Table 2**, all the compression properties of the cylindrical cores were evaluated considering the cross-sectional area of the cap, although not for all the cores localized cracks along the outer edges of the cap were reported. In the case of literature data, this may differ from the procedure adopted in the original paper. The grey cells in **Table 2** identify the values excluded from the correlation study in agreement with the observations made in Section 3.2. Consequently, the analysis is here performed considering only single wythe specimens.

Using a linear regression analysis, the relation between compression properties of the cores and of the wallets is presented in **Fig. 14**. The compressive strength ($f'_{m,core}$), the Young's modulus (E_{core}), peak strain ($\varepsilon_{peak,core}$) and the compressive fracture energy ($G_{f\text{-}c,core}$) obtained by core testing are plotted against the same properties obtained by tests on companion specimens (f'_m, E, ε_{peak}, $G_{f\text{-}c}$). In each graph, the results for T-shaped cores (100 mm in diameter) are indicated with yellow markers and those for H-shaped cores with blue markers; in the case of CS masonry, partially black markers are adopted to distinguish them from clay masonry specimens. For every object, the standard deviation of the properties for the core is given with a horizontal bar, while for the wallets with a vertical bar. The red dashed line shows a one-to-one correlation curve, while the grey area gives the scatter band.

Comparing the results of the companion specimens and of the cores, a very good correlation is found in terms of compressive strength and Young's modulus. A ratio equal to 0.99 with a correlation coefficient of 0.88 is obtained for the compressive strength (**Fig. 14**a). Similarly, a ratio equal to 1.05 with a correlation coefficient of 0.92 is obtained for the Young's modulus (**Fig. 14**b). For the compressive strength, the coefficient of variation was similar in the case of tests on cores and wallets, with a maximum of 21%. For the Young's modulus, wallets as well as cores from existing clay masonry object (Rengersweg) showed the highest values of standard deviation, which may

be attributed to spatial variability of masonry properties caused by workmanship and aging. The results obtained from both T-shaped cores (with 100 mm in diameter) and H-shaped ones (with 150 mm in diameter) show a good correlation with wallets. Consequently, for the analyzed cases, no size effect is reported in the evaluation of compressive strength and the Young's modulus. This conclusion is in line with findings by Van Mier [8], where compressive strength and Young's modulus of the concrete cubes having different heights were similar and independent of the specimen size.

Regarding the peak strain and the compressive fracture energy, no clear correlation is found between results of tests on cores and tests on wallets. The correlations improve if the T-shaped cores with 100 mm and the H-shaped cores with 150 mm in diameter are treated separately. Lower values of peak strain and higher values of fracture energy are obtained by tests on wallets with respect to the core testing method. The peak strain value obtained for the wallets is 0.80 times the one for the T-shaped cores and 0.55 times the one for the H-shaped cores. The compressive fracture energy for the wallets is 2.72 times of the one for the T-shaped cores and 1.73 times of the one for the H-shaped cores. Considering the energy per normalized unit of area (specific energy), it will be expected that a higher value of specific energy is needed to crack and crush small-diameter masonry cores rather than larger companion specimens.

In conclusion, despite the differences between the boundary conditions of the companion wallets and of the cores (due to the confinement effect of the capping mortar), the complete nonlinear response of existing masonry structures can be evaluated. The compressive strength and the Young's modulus obtained from the cores show very good correlations with the properties obtained from the companion specimens. Independently on the core size (i.e. cores with diameter of 150 or 100 mm), a correlation factor of one is found with a high correlation coefficient. No clear correlation could be found for the peak strain and the compressive fracture energy obtained from tests on cores and companion specimens. A dependency on the specimen size is observed in this study, which could however be influenced by the limited number of considered objects. Further studies are necessary for the evaluation of the post-peak softening properties.

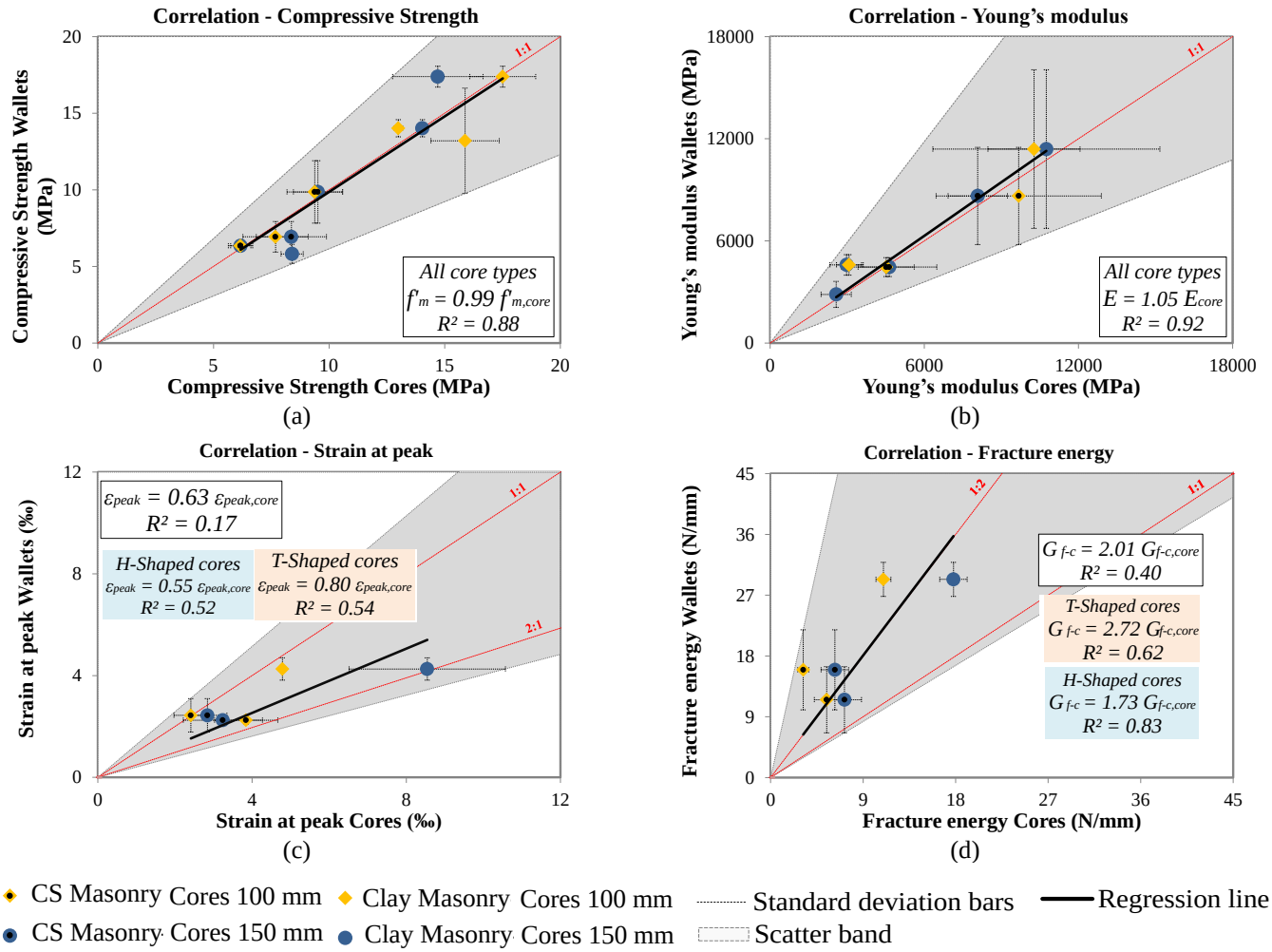

Fig. 14. Correlation between compression properties of the single wythe cylindrical cores and of the companion specimens: (a) compressive strength; (b) Young's modulus; (c) peak strain; (d) compressive fracture energy.

Considering the good correlations obtained for different test methods in terms of compressive strength and Young's modulus, the database is further used to obtain correlations between these two masonry properties. **Fig. 15** gives the relation between the Young's modulus and the compressive strength using mean values of the properties. Considering all the values obtained from both testing methods (excluding data marked in grey in **Table 2**), a ratio between Young's modulus and compressive strength equal to 545 with a low correlation coefficient of 0.35 is found. Approximately, the same factor is found if cores and wallets are treated separately. Dutch national annex [31] and Eurocode 6 [46] proposed an empirical linear formula in which the ratio between Young's modulus and characteristic compressive strength is equal to 700 and 1000, respectively. Note that in this study, the values of characteristic compressive strength are not reported, since in the case of exiting objects only three wallets were tested.

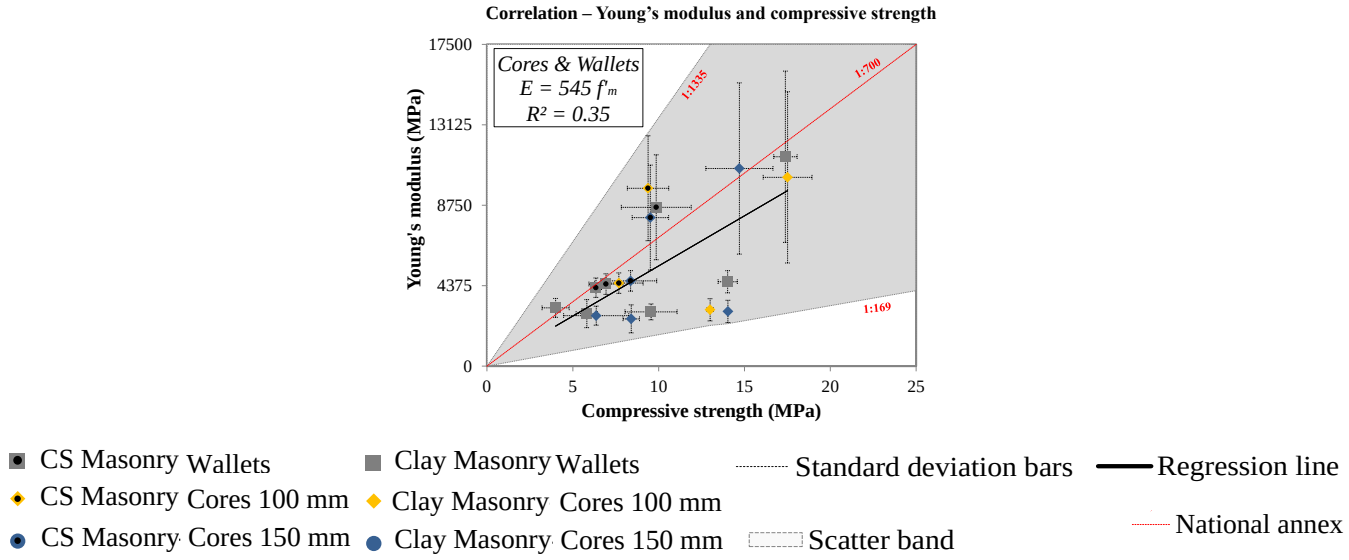

Fig. 15. Correlation among the mean values of Young's modulus and the mean values of compressive strength obtained from both testing methods, excluding data marked grey in **Table 2**.

5 Conclusions

This paper illustrates and discusses the suitability of the test on small-diameter cores to evaluate the nonlinear behavior of masonry in compression. This testing method is classified as being slightly-destructive, as extraction of 150 mm (H-shaped) or 100 mm (T-shaped) diameter samples does not cause any disruption of the building functionality. Seven masonry objects were selected either replicated in the laboratory or extracted from existing buildings. Differently than previous studies, the present work was not limited to the evaluation of the compressive strength and the Young's modulus, but also aimed at characterizing the full nonlinear stress-strain behavior including post-peak softening. The Young's modulus, compressive strength and corresponding strain, compressive fracture energy as well as the stress-strain relationship were established. To validate the accuracy of results from the core tests, a comparative experimental approach was adopted by performing tests on companion wallets. The database established from tests on cores and tests on companion wallets was further augmented and expanded by literature data. The focus was on the correlation between the compression properties obtained from tests on cores and companion specimens made of single wythe brick masonry. The following conclusions can be drawn:

1 Due to the higher stiffness of the capping mortar, the lateral deformation of the masonry is restrained. Thus, tensile cracking of the capping mortar cannot be avoided due to arising the horizontal compressive stress in the masonry and the horizontal tensile stress in the capping mortar. Further experimental and numerical studies are suggested to investigate the influence of cap stiffness and cap geometry on compression properties.

2 Masonry under compressive load shows a nonlinear behavior caused by a complex interaction among the masonry constituents (e.g. masonry units and mortar joint) each having different elastic properties. Upon increasing load, diffused micro-cracks grow and coalesce into macro-cracks resulting in localization of deformations and thus masonry failure. The majority of core specimens showed only formation of out-of-

plane splitting cracks and debonging cracks across the length. In addition, localized cracks formed along the end boundaries of the cap eventually leading to the detachment of the marginal parts of the cores. Crushing and degrading of the inner part of the cores were also observed. On the contrary, the wallets showed a complex crack pattern with damage distributed across both length and width. Considering the localization of the cracks near the cap end boundaries, it is suggested to evaluate the compression properties obtained by core testing considering stress evaluated with respect to the cap cross-sectional area.

3 Despite the difference in crack pattern, the compressive stress-strain relationships obtained from cores and wallets showed remarkable similarity. They were characterized by a linear-elastic branch followed by a hardening behavior until the peak and a post-peak softening behavior, which can be approximated by a linear descending branch, until a residual strength of 5-10% of the compressive strength.

4 By comparing the two tests methods, a one-to-one correlation (with correlations coefficient higher than 0.88) is obtained in terms of both compressive strength and Young's modulus. The strong correlations, which could be established only for single wythe masonry, are independent on the masonry types (calcium silicate or clay masonry) and core size (i.e. cores with 150 and 100 mm in diameter). In light of the latter finding, the use of smaller diameter cores is preferable as the damage caused by extraction is less visible and can be easily repaired.

5 The core testing method tends to overestimate the values of the peak strain, while, it underestimates the evaluation of the compressive fracture energy. The differences in the post-peak response of the cores and wallets were also detected in terms of crack patterns, as cores showed no or limited in-plane splitting cracks and more widening of previously formed cracks rather than developing new cracks at close spacing. In addition, generally, higher values of the compressive fracture energy are reported from tests on H-shaped cores with respect to the T-shaped ones. However, no specific trend is observed in terms of peak strain of both core types. As a function of the core size, the strain corresponding to the peak stress as well as the compressive fracture energy of the single wythe cylindrical cores is only slightly correlated to the corresponding properties of the companion wallets. It should be noted that these correlations are obtained for a restricted data set that account separately for the core size. To clarify this size effect and the confining effect of the cap on the compression properties of the cores, more studies are suggested.

6 Aiming to predict the mean values of the Young's modulus based on the mean values of the compressive strength of the corresponding object, a regression analysis was performed including results of both testing methods. A linear relation with a factor equal to 545 is found, with a low correlation coefficient of 0.35.

In conclusion, the comparative experimental study demonstrates the great suitability of the core testing method for addressing both compressive strength and Young's modulus. Moreover, the core testing method shows potential for estimation of peak strain and compressive fracture energy. From a comparison with conventional testing methods, it can be concluded that the core testing method is less invasive than tests on wallets, but can provide comparable results; additionally, it employs conventional equipment reducing the technical challenges of current in-

situ tests methods, e.g. flat-jack tests . However, further studies, both experimentally and numerically, are suggested to investigate the effect of boundary conditions as well as the confinement effect of capping mortar on the evaluation of the compression properties.

Acknowledgment

This research was funded by Nederlandse Aardolie Maatschappij (NAM), under contract numbers UI46268 “Physical testing and modelling – Masonry structures Groningen” (contract holders Jan van Elk and Jeroen Uilenreef) and UI63654 “Testing program 2016 for Structural Upgrading of URM Structures” (contract holders Dick den Hertog and Reza Sarkhosh), which is gratefully acknowledged. The authors are thankful to the staff of the TU Delft Macrolab/Stevinlaboratory and to M.Sc. students Lucia Licciardello and Elena Casprini for assistance during the tests. The collaboration with engineering company ARUP for extracting samples is acknowledged. The authors acknowledge the collaboration with Dr Ad Vermeltfoort and Prof. Dirk Martens from Eindhoven University of Technology, who performed compression tests on wallets extracted from Molenweg building, and the collaboration with engineering company B|A|S, who performed compression tests on wallets extracted from Rengersweg building.

Access to experimental data

The experimental results of the presented tests are available via the 4TU.ResearchData repository at https://doi.org/10.4121/uuid:5bb2c901-9b1b-4a43-a2fe-11cd3d1d0c52. The data are distributed under the license type CC BY.

References

[1] Haller P. Load capacity of brick masonry. Designing, engineering and constructing with masonry products. 1969:129-49.
[2] Lenczner D. Elements of load bearing brickwork. International Series of Monograms in Civil Engineering, Vol. 5: Pergamon Press, New York; 1972.
[3] Hendry AW. Structural brickwork. London: Macmillan; 1998 Nov 11.
[4] Rots JG. Numerical simulation of cracking in structural masonry. Heron. 1991;36(2):49-63.
[5] Lourenço PJBB. Computational strategies for masonry structures: Delft University of Technology; 1997.
[6] Vermeltfoort AT. Brick-mortar interaction in masonry under compression: Technische Universiteit Eindhoven; 2005.
[7] Lourenço PJBB, Pina-Henriques J. Validation of analytical and continuum numerical methods for estimating the compressive strength of masonry. Computers & structures. 2006;84(29-30):1977-89.
[8] Van Mier JGM. Strain-softening of concrete under multiaxial loading conditions: Technische Hogeschool Eindhoven Eindhoven; 1984.
[9] Vonk RA. Softening of concrete loaded in compression: Technische Universiteit Eindhoven; 1992.
[10] Bažant ZP, Xiang Y. Size effect in compression fracture: splitting crack band propagation. Journal of engineering mechanics. 1997;123(2):162-72.
[11] EN 1052-1. Methods of test for masonry - Part 1: Determination of compressive strength. 1998.
[12] ASTM C 1197-04. Standard test method for in-situ measurement of masonry deformability properties using the flat jack method. 2004.
[13] Binda L, Tiraboschi C. Fiat-Jack Test: A slightly destructive technique for the diagnosis of brick and stone masonry structures. Restoration of Buildings and Monuments. 1999;5(5):449-72.
[14] Cescatti E, Dalla Benetta M, Modena C, Casarin F, editors. Analysis and evaluations of flat jack test on a wide existing masonry buildings sample. 16th Brick & Block Masonry Conference; 2016 26-30 June; Padova, Italy. London, UK: CRC Press.
[15] Jafari S, Esposito R, Rots GJ, editors. A Comparative study on the evaluation of different testing techniques: Evaluating the mechanical properties of masonry. 10th International Masonry Conference; 2018 9-11 July; Milan, Italy.
[16] Noland J, Kingsley G, Atkinson R, editors. Utilization of nondestructive techniques into the evaluation of masonry. 8th International Brick/Block Masonry Conference; 1988 19-21 September; Dublin, Ireland.
[17] de Vekey R. A review of the work of the RILEM committee 127-MS: testing masonry materials and structures. Materials and Structures. 1997;30(1):12-6.
[18] Brencich A, Sterpi E, editors. Compressive strength of solid clay brick masonry: Calibration of experimental tests and theoretical issues. 5th Structural Analysis of Historical Constructions; 2006 06-08 November; New Delhi, India: Macmillan India Ltd.

[19] Brencich A, Sabia D. Experimental identification of a multi-span masonry bridge: The Tanaro Bridge. Construction and Building Materials. 2008;22(10):2087-99.

[20] Ispir M, Demir C, Ilki A, Kumbasar N. Material characterization of the historical unreinforced masonry Akaretler row houses in Istanbul. Materials in Civil Engineering. 2009;22(7):702-13.

[21] Sassoni E, Mazzotti C. The use of small diameter cores for assessing the compressive strength of clay brick masonries. Journal of Cultural Heritage. 2013;14(3):e95-e101.

[22] Sassoni E, Mazzotti C, Pagliai G. Comparison between experimental methods for evaluating the compressive strength of existing masonry buildings. Construction and Building Materials. 2014;68:206-19.

[23] Pelà L, Canella E, Aprile A, Roca P. Compression test of masonry core samples extracted from existing brickwork. Construction and Building Materials. 2016;119:230-40.

[24] Jafari S, Esposito R, Rots GJ, editors. Literature review on the assessment of masonry properties by tests on core samples. 4th WTA International PhD Symposium; 2017 14-16 September; Delft, Netherlands: WTA Nederland - Vlaanderen.

[25] Segura J, Pelà L, Roca P, editors. Influence of geometry of cylindrical samples in the mechanical characterization of existing brickwork. 11th International Conference on Structural Analysis of Historical Constructions; 2019: Springer.

[26] Rots JG, Messali F, Esposito R, Mariani V, Jafari S. Multi-Scale Approach towards Groningen Masonry and Induced Seismicity. Key Engineering Materials. 2017;747:653-61.

[27] UIC 778-3R. Recommendations for the assessment of the load carrying capacity of the existing masonry and mass-concrete arch bridges. 1995.

[28] Jafari S, Rots JG, Esposito R, Messali F. Characterizing the material properties of dutch unreinforced masonry. Procedia engineering. 2017;193:250-7.

[29] Zapico Blanco B, Tondelli M, Jafari S, Graziotti F, Millekamp H, Rots GJ, et al., editors. A masonry catalogue for the Groningen region. Proceedings of the 16th European Conference on Earthquake Engineering; 2018 18-21 June; Thessaloniki, Greece.

[30] Messali F, Esposito R, Jafari S, Ravenshorst G, Korswagen P, Rots J, editors. A multiscale experimental characterisation of Dutch unreinforced masonry buildings. Proceedings of 16th European Conference on Earthquake Engineering; 2018 18-21 June; Thessaloniki, Greece.

[31] NPR 9998 Assessment of structural safety of buildings in case of erection, reconstruction and disapproval: Basis rules for seismic actions: Induced earthquakes (partially in Dutch). 2017.

[32] Graziotti F, Penna A, Magenes G. A comprehensive in situ and laboratory testing programme supporting seismic risk analysis of URM buildings subjected to induced earthquakes. Bulletin of Earthquake Engineering. 2018:1-25.

[33] Damiola M, Esposito R, Messali F, Rots JG, Milani G, Taliercio A, et al., editors. Quasi-static cyclic two-way out-of-plane bending tests and analytical models comparison for URM walls; 2018 9-11 July; Milan, Italy.

[34] Messali F, Rots GJ. In-plane drift capacity at near collapse of rocking unreinforced calcium silicate and clay masonry piers. Engineering Structures. 2018;164:183-94.

[35] Esposito R, Terwel K, Ravenshorst G, Schipper H, Messali F, Rots GJ, editors. Cyclic pushover test on an unreinforced masonry structure reseambling a typical Dutch terraced house. 16th World Conference on Earthquake; 2017 9-13 January; Santiago, Chile.

[36] ASTM C1532. Standard practice for selection, removal, and shipment of masonry assemblage specimens from existing construction.

[37] EN 1015-11. Method of test for mortar for masonry – Part 11: Determination of flexural strength of hardened mortar. 1999.

[38] NEN 6790. Technical principles for building structures - TGB 1990 - Masonry structures - Basic requirements and calculation methods. 2005.

[39] EN 772-1. Methods of test for masonry units - Part 1: Determination of compressive strength. 2000.

[40] EN 13412. Products and systems for the protection and repair of concrete structures. Test methods. Determination of Modulus of Elasticity in Compression. 2007.

[41] ASTM C1552 − 16. Practice for Capping Concrete Masonry Units, Related Units and Masonry Prisms for Compression Testing. 2016.

[42] García D, San-José JT, Garmendia L, Larrinaga P. Comparison between experimental values and standards on natural stone masonry mechanical properties. Construction and Building Materials. 2012;28(1):444-9.

[43] Augenti N, Parisi F. Constitutive models for tuff masonry under uniaxial compression. Journal of Materials in Civil Engineering. 2010;22(11):1102-11.

[44] Vermeltfoort AT. Tests for the characterization of original Groningen masonry under compression and shear loading.

[45] Nonnekes SM. Masonry Research Report Location: Rengersweg 11, 9908 PL, Godlinze. Venlo, Netherlands: Research & Technology B|A|S, 2015 15 April.

[46] EN B. 1-1: 2005 Eurocode 6: Design of masonry structures—General rules for reinforced and unreinforced masonry structures. 1996.